Journal of Alloys and Compounds 509 (2011) 5042–5046

Contents lists available at ScienceDirect

Journal of Alloys and Compounds

journal homepage: www.elsevier.com/locate/jallcom

High-field magnetization of a $Dy_2Fe_{14}Si_3$ single crystal

A.V. Andreev[a,*], M.D. Kuz'min[b], S. Yoshii[c], E.A. Tereshina[a,c], K. Kindo[d], M. Hagiwara[e], F.R. de Boer[f]

[a] Institute of Physics ASCR, Na Slovance 2, 18221 Prague, Czech Republic
[b] Leibniz-Institut für Festkörper- und Werkstoffforschung, PF 270116, 01171 Dresden, Germany
[c] Institute for Materials Research, Tohoku University, Katahira 2-1-1, Sendai 980-8578, Japan
[d] Institute for Solid State Physics, University of Tokyo, 5-1-5 Kashiwanoha, Kashiwa, Chiba 277-8581, Japan
[e] KYOKUGEN, Osaka University, Toyonaka, Osaka 560-8531, Japan
[f] Van der Waals-Zeeman Institute, University of Amsterdam, Postbus 94485, 1090 GL Amsterdam, The Netherlands

ARTICLE INFO

Article history:
Received 4 January 2011
Received in revised form 31 January 2011
Accepted 2 February 2011
Available online 4 March 2011

Keywords:
Rare-earth intermetallics
R_2T_{17}
High magnetic fields
Field-induced transition
Metamagnetism
Magnetic anisotropy

ABSTRACT

The magnetization of a $Dy_2Fe_{14}Si_3$ single crystal was measured at 4.2 K in pulsed fields up to 51 T along the principal axes. The compound orders ferrimagnetically at 500 K, has a spontaneous magnetic moment of 8 μ_B/f.u. (at 4.2 K) and exhibits a very large magnetic anisotropy, ⟨1 0 0⟩ being the easy axis. In fields applied along the ⟨1 0 0⟩ and ⟨1 2 0⟩ axes, field-induced phase transitions are observed at 33 T and at 39 T, respectively. The *c*-axis magnetization curve crosses the easy-axis curve at 19 T. At higher fields, for all directions, the magnetization continues to increase due to further bending of the sublattice moments. Temperature evolution of magnetic anisotropy and magnetic hysteresis are discussed as well.

1. Introduction

Dy_2Fe_{17} belongs to the R_2T_{17} family of rare-earth (R = Ce–Lu) intermetallic compounds with late 3d transition metals T. It has the hexagonal crystal structure of the Th_2Ni_{17} type characteristic for heavy R. As found from single-crystal measurements, the spontaneous magnetic moment M_s = 16.8 μ_B/f.u. (per formula unit) in the ground state is located in the basal plane along the *a* axis [1–3]. The compound is a collinear ferrimagnet. In such compounds, field-induced phase transitions are expected from the collinear ferrimagnetic structure through canted structure to final collinear ferromagnet. This has indeed observed in Ho_2Co_{17} [4] and later been shown to occur in many other ferrimagnetic R_2Fe_{17} and R_2Co_{17} compounds with easy-plane type of anisotropy. The high-field magnetic transitions, that take place in these compounds if the field is applied within the basal-plane directions, are based on the competition between the Zeeman energy (strength of the applied field) and the strength of the 4f–3d exchange interaction. For Dy_2Fe_{17}, the transitions at 54 T for magnetic field *H* along the *a*-axis [1 0 0] and at 70 T along the *b*-axis [1 2 0] have been predicted [5]. To observe both transitions, one needs magnetic field up to 75 T which is currently not available for magnetization measurements of metallic systems. However, if the strength of the intersublattice coupling is reduced, for example, by dilution of the Fe sublattice, the transitions can be observed at still high but achievable fields.

A study of the Si solid solutions in R_2Fe_{17}, $R_2Fe_{14}Si_3$, performed on polycrystalline samples [6], has revealed a strong modification of both the intra- and inter-sublattice interactions compared to R_2Fe_{17}. The effect is rather complicated, because the Fe-sublattice moment is weakened by the dilution with the non-magnetic Si, whereas the Fe–Fe exchange interaction is unexpectedly enhanced (T_C is 370 K in Dy_2Fe_{17} and 500 K in $Dy_2Fe_{14}Si_3$). Our single-crystal study of $Dy_2Fe_{14}Si_3$ [7] has shown that the transition fields indeed decrease, to 33 and 39 T, along the *a* and *b* axis, respectively. In the present paper we show experimental results in more detail and perform their theoretical analysis absent in [7].

2. Experimental

The single crystal of $Dy_2Fe_{14}Si_3$ of 20 mm length and 4 mm diameter has been grown by a modified Czochralski method in a tri-arc furnace from a stoichiometric mixture of the pure elements (99.9% Dy, 99.98% Fe and 99.999% Si). The lattice parameters determined by X-ray powder diffraction, *a* = 840.8 pm, *c* = 826.8 pm, are in good agreement with the literature [6]. The magnetization was measured along the [1 0 0] (*a*), [1 2 0] (*b*) and [0 0 1] (*c*) axes by extraction method in steady fields up to 5 T at 4.2–300 K using a commercial SQUID magnetometer (Quantum Design). The high-field magnetization has been measured in the Center for Quantum Science and Technology under Extreme Conditions (KYOKUGEN) at Osaka University, at pulsed

* Corresponding author at: Institute of Physics ASCR, Na Slovance 2, 18221 Prague, Czech Republic. Tel.: +420 221912735.
E-mail addresses: andreev@mag.mff.cuni.cz, a.andreev@seznam.cz (A.V. Andreev).

0925-8388/$ – see front matter © 2011 Elsevier B.V. All rights reserved.
doi:10.1016/j.jallcom.2011.02.012

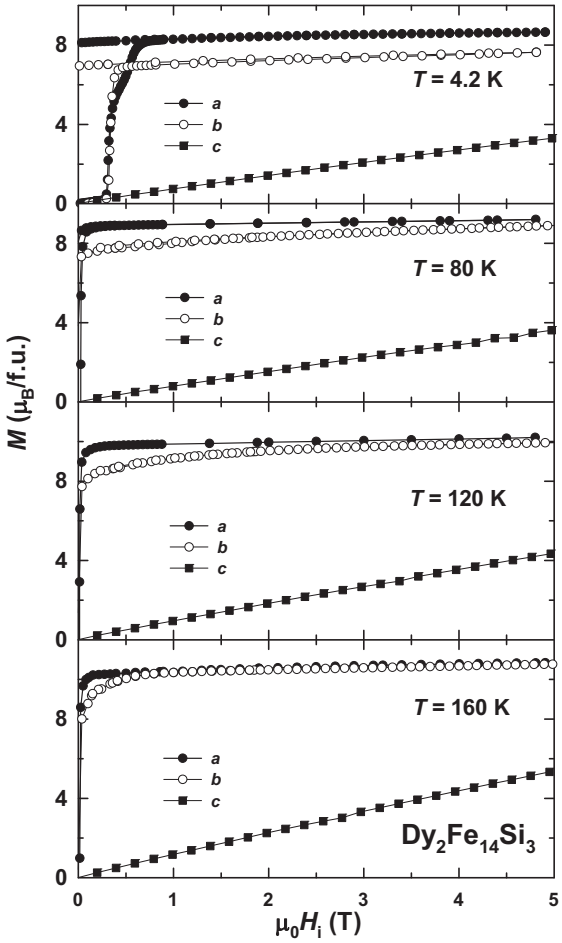

Fig. 1. Magnetization curves of a $Dy_2Fe_{14}Si_3$ single crystal measured along the principal axes at T = 4.2–160 K.

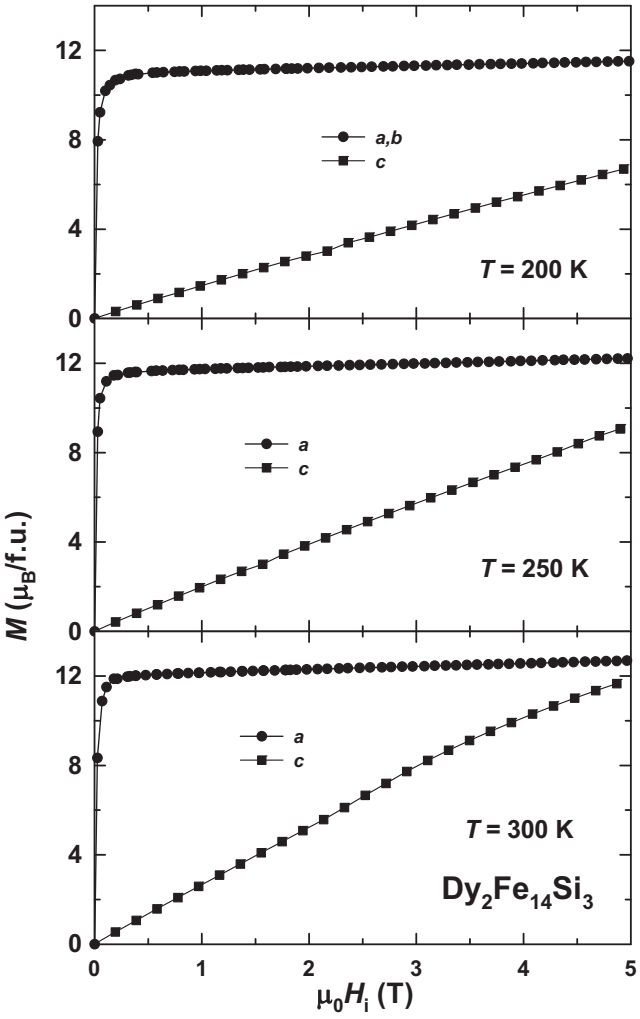

Fig. 2. The same as Fig. 1, for T = 200–300 K.

fields up to 52 T with pulse duration of 20 ms at 4.2 K. The magnetization curves presented in this paper have been corrected for demagnetizing field.

3. Results and discussion

Figs. 1 and 2 show the magnetization curves measured along the principal axes at different temperatures. It is seen that $Dy_2Fe_{14}Si_3$ is a highly anisotropic ferrimagnet with the easy *a* axis. The ferrimagnetic arrangement of the Dy and Fe sublattices is manifest in Figs. 1 and 2, where M_S grows with temperature. It is also seen in Fig. 3, where temperature dependence of magnetization of $Dy_2Fe_{14}Si_3$ in 1 T measured along the easy axis is compared with that for $R_2Fe_{14}Si_3$ with non-magnetic Y and Lu [8]. The magnetic isotherm measured with the field applied along the *a*-axis exhibits M_S = 8 μ_B/f.u. at 4.2 K. If one subtracts this value from M_S = 26 μ_B/f.u. for $Y_2Fe_{14}Si_3$, which can be considered as the magnetic moment of the Fe sublattice M_{Fe} in $Dy_2Fe_{14}Si_3$, the magnetic moment of the Dy sublattice M_{Dy} is equal to 18 μ_B/f.u., in fair agreement with 2 free-ion values of Dy^{3+} (20 μ_B).

As seen from Figs. 1 and 2, a pronounced anisotropy within the basal plane vanishes above 160 K, where the *b* and *a* axis magnetization curves coincide. The anisotropy between the basal plane and the *c* axis persists at much higher temperatures; the anisotropy field still exceeds 5 T at 300 K.

At low temperatures, the basal-plane magnetization curves of $Dy_2Fe_{14}Si_3$ exhibit a characteristic strong hysteresis with a very low initial susceptibility, an abrupt saturation in narrow field inter-

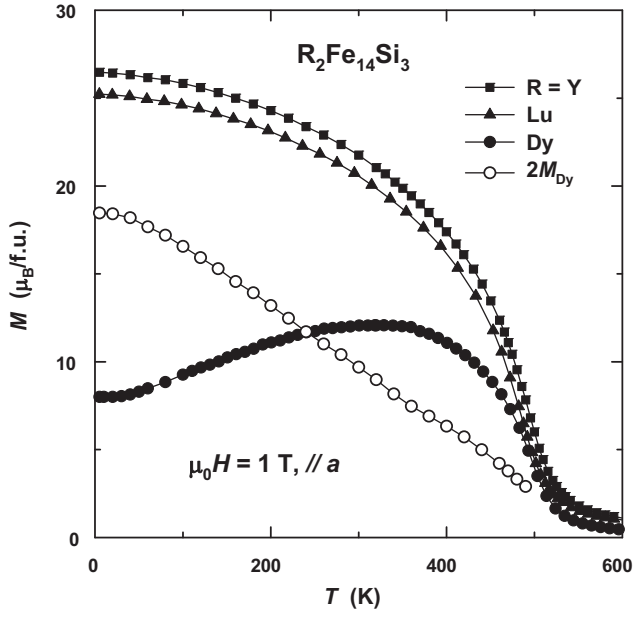

Fig. 3. Temperature dependence of magnetization of $R_2Fe_{14}Si_3$ single crystals measured along the *a* axis in field of 1 T.

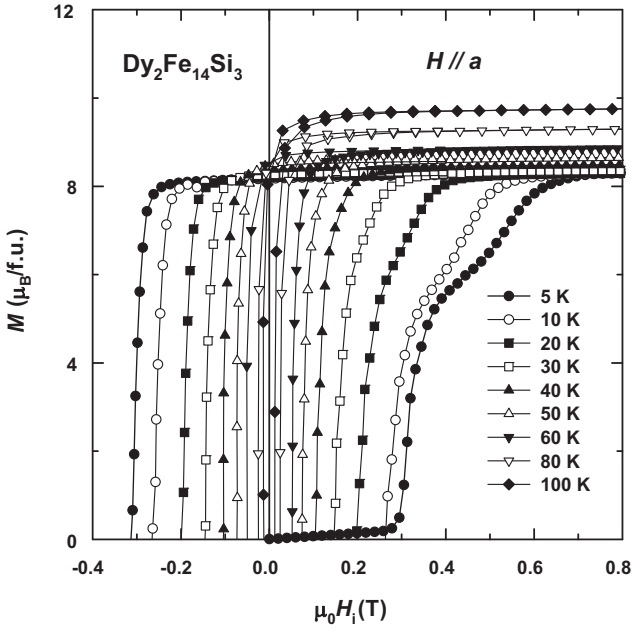

Fig. 4. Hysteresis loops measured along the *a* axis at different temperatures.

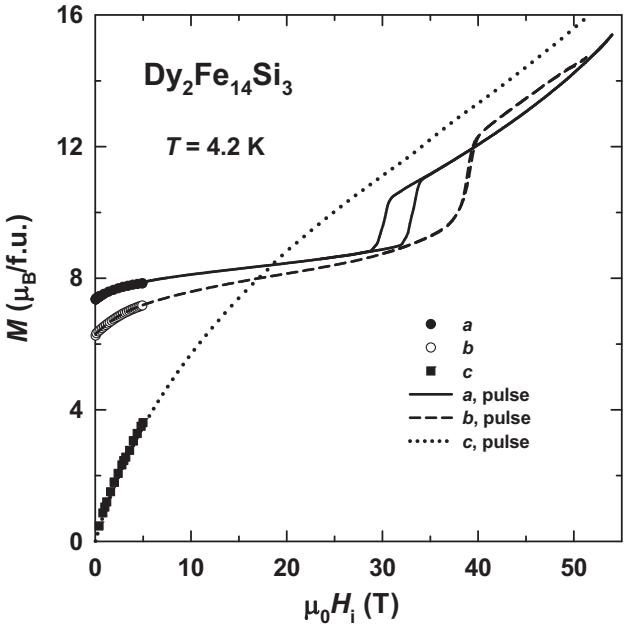

Fig. 6. Magnetization curves of a $Dy_2Fe_{14}Si_3$ single crystal measured along the principal axes in pulsed magnetic fields at 4.2 K (lines). The symbols represent steady-field results.

val, rectangular hysteresis loops (Fig. 4) and a drastic exponential decrease of coercive field with increasing temperature (Fig. 5). All these features agree well with the model of high intrinsic coercivity of narrow domain walls applicable to highly anisotropic magnets at low temperatures. However, the easy-plane type of magnetic anisotropy is usually not strong enough to provide the domain-wall width of the order of several interatomic distances needed for the effective domain-wall pinning in the framework of this model. Then, such a hysteresis is not observed in Dy_2Fe_{17} without Si, whereas the magnetization and anisotropy of Dy_2Fe_{17} and $Dy_2Fe_{14}Si_3$ differ only quantitatively. The same situation occurs in the $Tb_2Fe_{17-x}Si_x$ compounds: a strong hysteresis appears only in the crystals with Si [9]. On our opinion, the effective domain-wall pinning in $R_2Fe_{17-x}Si_x$ with multiaxial (e.g., easy-plane) magnetic anisotropy originates from the concentration inhomogeneities at the microscopic level, which are always present in quasibinary systems.

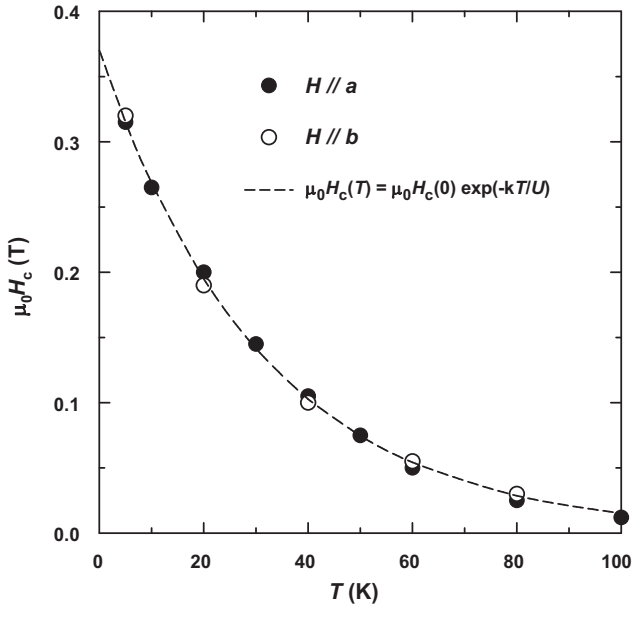

Fig. 5. Temperature dependence of coercive field measured along the *a* and *b* axes. The dashed line represents the fit with parameters $\mu_0 H_c(0) = 0.37$ T, $U = 43 \times 10^{-23}$ J.

Fig. 6 shows high-field magnetization curves at $T = 4.2$ K. The *c*-axis curve crosses the easy-axis *a*-curve at 19 T. If this value is regarded as the anisotropy field H_a, the corresponding uniaxial anisotropy energy E_a amounts to 3.2 MJ m^{-3} (58 K/f.u.). The *c*-axis magnetization, however, continues to grow smoothly above 19 T, no phase transition taking place at this point. Such a behavior is characteristic of strongly anisotropic ferrimagnets magnetized in a hard direction [10]. In this case the notion of anisotropy field is not meaningful, because the magnetization process consists of not only rotation of the total magnetic moment toward the field direction but also of field-induced non-collinearity of the ferrimagnetically coupled sublattices.

In the field range from 30 to 33 T, the *a*-axis magnetization exhibits a strongly hysteretic transition. A similar, but much less hysteretic transition is found at about 39 T if the field is applied in the *b*-axis direction, the hard magnetization direction in the easy plane. If the general interpretation is applied to the *a*-axis magnetization of $Dy_2Fe_{14}Si_3$, it means that the low-field collinear magnetic structure, in which the Dy moments lie along the *a* axis in the basal plane, antiparallel with the Fe moments, is broken around 30–33 T and a transition takes place to a moment configuration in which the Dy moments jump to another easy direction and in which Zeeman energy is gained at the expense of intersublattice exchange energy.

Fig. 7 displays theoretical magnetization curves along the three principal axes up to field-induced ferromagnetic state. The starting point for the calculations was the following non-equilibrium thermodynamic potential [11]:

$$\Phi = \lambda M_{Fe} \bullet M_{Dy} - (M_{Fe} + M_{Dy}) \bullet H + E_a \quad (1)$$

here the first term describes the Fe–Dy exchange, $\lambda > 0$, while the second one describes Zeeman's interaction with applied magnetic field. The last term is the anisotropy energy; in general, it depends on orientations of both sublattice vectors, M_{Fe} and M_{Dy}, with respect to the crystal axes. In this work, however,

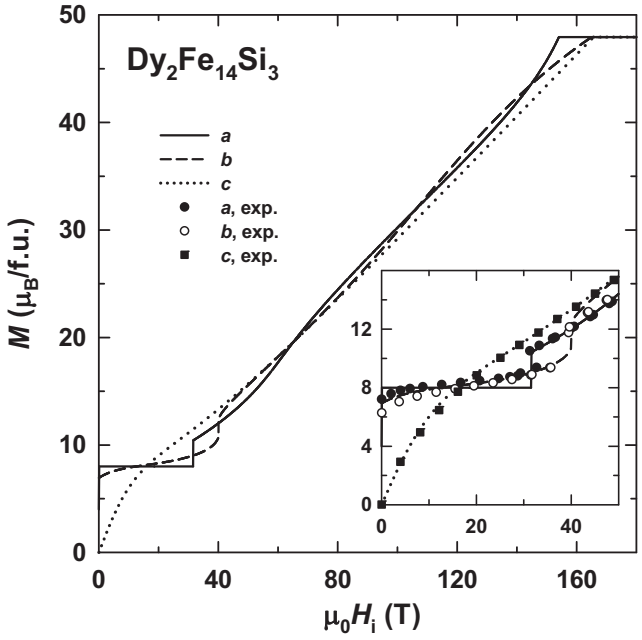

Fig. 7. Calculated magnetization curves of a $Dy_2Fe_{14}Si_3$ single crystal along the principal axes. Inset: comparison of fits and experimental data at 4.2 K (symbols).

the dependence on M_{Fe} is neglected because the corresponding anisotropy energy is small, ~1 MJ m^{-3}, as known from $R_2Fe_{14}Si_3$ with non-magnetic R [8]. Our consideration is limited to low temperatures, so we assume for the magnetic moment of the Dy sublattice $|M_{Dy}| = M_{Dy} = \text{const.} = 20\ \mu_B$/f.u., i.e. it is taken equal to the free-ion value. The moment of the Fe sublattice is ascribed to the difference between the total moment and $|M_{Dy}|$: $|M_{Fe}| = M_{Fe} = \text{const.} = 28\ \mu_B$/f.u. We find it convenient to introduce the following dimensionless quantities:

$$\varphi = \frac{\Phi}{\lambda M_{Fe}^2}, \qquad h = \frac{H}{\lambda M_{Fe}}, \qquad m = \frac{M_{Dy}}{M_{Fe}}, \qquad \varepsilon_a = \frac{E_a}{\lambda M_{Fe}^2} \tag{2}$$

Denoting as α and β the angles between the applied magnetic field and the Fe- and Dy-sublattice moments, respectively, we rewrite the thermodynamic potential (1) as follows:

$$\varphi(\alpha, \beta) = m\cos(\alpha + \beta) - h\cos\alpha - mh\cos\beta + \varepsilon_a(\beta) \tag{3}$$

in accordance with the above, the anisotropy energy depends on β but not on α. The specific form of this dependence is dictated by the orientation of applied magnetic field.

$$H||a, b : \varepsilon_a(\beta) = \pm\kappa_4 \cos 6\beta \tag{4}$$

with

$$\kappa_4 = \frac{|K_4|}{\lambda M_{Fe}^2} \tag{5}$$

where K_4 is the conventional basal-plane anisotropy constant of the hexagonal crystal. The upper (lower) sign in Eq. (4) corresponds to H pointing in the hard (easy) magnetization direction in the basal plane.

$$H||c : \varepsilon_a(\beta) = \kappa_1 \sin^2\beta \tag{6}$$

with

$$\kappa_1 = \frac{K_1}{\lambda M_{Fe}^2} \tag{7}$$

K_1 being the conventional first anisotropy constant of the hexagonal crystal. Allowing for higher-order anisotropy constants, K_2 and/or K_3, proved unnecessary. Their effect on the magnetization curves was found to be insignificant.

The calculation of the magnetization curves consisted in minimizing the function $\varphi(\alpha,\beta)$, Eq. (3), for a given h and substituting the obtained equilibrium orientation angles α and β into an expression for reduced magnetization,

$$\sigma = \frac{\cos\alpha + m\cos\beta}{1 - m} \tag{8}$$

for $H||a,b$ the minimization was carried out numerically, following the simple algorithm given in Ref. [11]. In the case of $H||c$ parametric expressions for σ vs. h were used, Eqs. (15) and (16) of Ref. [10]. In order to convert the obtained dependence $\sigma(h)$ to $M(H)$, the ordinates have to be multiplied by the known spontaneous moment, $M_s = 8\ \mu_B$/f.u., and the abscissas by the molecular field on Dy, λM_{Fe}. The latter is evaluated by the method proposed in Ref. [11]: knowing the relative height of the magnetization jump at $\mu_0 H_1 = 31.5$ T, $\Delta\sigma_1 = 0.32$, one finds from Eq. (14) of Ref. [11] the corresponding dimensionless critical field, $h_1 = 0.34$. Then $\lambda M_{Fe} = \mu_0 H_1/h_1 = 93$ T.

Eq. (3) contains model parameters of two kinds: whereas the sublattice moments ratio m is a known quantity, $m = 20/28 = 0.714$, κ_1 and κ_4 are adjustable parameters. The magnetization curves are not particularly sensitive to the anisotropy constants, so these cannot be determined but rather approximately: $\kappa_1 = -0.04$ and $\kappa_4 = 0.002$, or $K_1 = -70$ K/f.u. and $K_4 = -3.5$ K/f.u.

4. Conclusions

Comparing the calculated magnetization curves with experiment (see Fig. 7, inset), one observes good agreement. The chosen model [11] seems to provide an adequate description of the high-field magnetization process in $Dy_2Fe_{14}Si_3$. One notes in particular that, according to the theoretical prediction, the magnetization jumps observed at 33 T and 39 T are the only ones and that further magnetization up to full saturation at about 160 T should proceed continuously. This is at variance with an earlier professed view [5] that a basal-plane magnetization curve of a hexagonal easy-plane ferrimagnet should always contain as many as three discontinuities. According to a more refined analysis [11], the number of discontinuities is determined by the strength of the basal-plane anisotropy in relation to the intersublattice exchange. This number can lie between zero in the case of extremely weak anisotropy and three in the strongly anisotropic case. In $Dy_2Fe_{14}Si_3$ one deals apparently with an intermediate case, with a single discontinuity in the magnetization curves along the a and b axes.

Acknowledgements

The work of A.V.A. and E.A.T. is a part of the research project AVOZ10100520 of Academy of Sciences of Czech Republic and has been supported by Czech Science Foundation (grant 202/09/0339). Scientific cooperation between the research groups of Czech Republic and Japan was supported by Japan Society for the Promotion of Science.

References

[1] A.V. Andreev, A.V. Deryagin, S.M. Zadvorkin, N.V. Kudrevatykh, V.N. Moskalev, R.Z. Levitin, Y.F. Popov, R.Y. Yumaguzhin, in: D.D. Mishin (Ed.), Fizika Magnitnykh Materialov (Physics of Magnetic Materials), 1985, pp. 21–49, Kalinin, (in Russian).
[2] S. Sinnema, Magnetic interactions in R_2T_{17} and $R_2T_{14}B$ intermetallic compounds, PhD Thesis, University of Amsterdam (1988).
[3] B. García-Landa, P.A. Algarabel, M.R. Ibarra, F.E. Kaizel, T.H. Ahn, J.J.M. Franse, J. Magn. Magn. Mater. 144 (1995) 1085.
[4] J.M.M. Franse, F.R. de Boer, P.H. Frings, R. Gersdorf, A. Menovsky, F.A. Muller, R.J. Radwanski, S. Sinnema, Phys. Rev. B 31 (1985) 4347.

[5] J.M.M. Franse, R.J. Radwanski, S. Sinnema, J. Phys. Colloq. 49 (1988) C8–C505.
[6] B.G. Shen, B. Liang, Z.H. Cheng, T.Y. Gong, H. Tang, F.R. De Boer, K.H.J. Buschow, Solid State Commun. 103 (1997) 71.
[7] E.A. Tereshina, A.V. Andreev, S. Yoshii, M.D. Kuz'min, F.R. de Boer, M. Hagiwara, K. Kindo, J. Phys.: Conf. Ser. 51 (2006) 147.
[8] A.V. Andreev, J. Alloys Comp. 475 (2009) 13.
[9] J. Du, J.H. Wu, C.C. Tang, Y.X. Li, W.S. Zhan, J. Appl. Phys. 84 (1998) 3305.
[10] M.D. Kuz'min, J. Magn. Magn. Mater. 323 (2011) 1068.
[11] M.D. Kuz'min, Y. Skourski, K.P. Skokov, K.-H. Müller, Phys. Rev. B 75 (2007) 184439.